Applied Thermal Engineering 90 (2015) 258–265

Contents lists available at ScienceDirect

Applied Thermal Engineering

journal homepage: www.elsevier.com/locate/apthermeng

Research paper

Numerical simulation of fast charge of natural gas on activated carbon in conjunction with variable velocity

J.C. Santos [a], J.M. Gurgel [b], F. Marcondes [c, *]

[a] Department of Mechanical Production Engineering, Regional University of Cariri, Av. Leão Sampaio, 107 – Juazeiro do Norte, Ceará 63040-000, Brazil
[b] Center of Alternative and Renewable Energy, Solar Energy Laboratory, Federal University of Paraiba, LES/UFPB – Cidade Universitária, João Pessoa, Paraíba 58090-900, Brazil
[c] Department of Metallurgical Engineering and Material Science, Federal University of Ceará, Campus do Pici, Bloco 714 Fortaleza, Ceará 60455-760, Brazil

HIGHLIGHTS

- The fast charge of methane in activated carbon is optimized.
- The gas adsorption is described by the mass, momentum, and energy balances.
- The effect of pressure drop and inlet temperature on charge dynamics is investigated.
- The results show that the mass transfer in the adsorbent has a great impact on the gas speed during the adsorption process.

ARTICLE INFO

Article history:
Received 24 March 2015
Accepted 28 May 2015
Available online 14 July 2015

Keywords:
Adsorbed natural gas
Fast charge
Activated carbon
Finite-volume method

ABSTRACT

This paper presents a numerical investigation of the dynamics of adsorption of pure methane in a packed column with activated carbon in order to optimize the fast charge process in adsorbed natural gas vessels. The investigation utilizes two main models. A model for the column that is described by mass, momentum, and energy balances in conjunction with the ideal gas equation and the monodisperse model for the adsorbent. The resulting equations are discretized by the finite-volume method. Several main findings were revealed from this investigation. Firstly, numerical results show that the mass transfer in the adsorbent has a great impact on the gas speed during the adsorption process. Secondly, the adsorbed mass of the column increases by reducing the gas inlet temperature. Lastly, it was observed that the saturation time in the column is a function of the applied pressure drop. In this case, the saturation time in the column varied between 500 and 1000 s. This range is considered satisfactory for the fast filling process of the column.

© 2015 Elsevier Ltd. All rights reserved.

1. Introduction

Recently, the main concern of researchers and environmentalists seem to center around the emissions of gases that cause global warming. That is, the carbon dioxide that results from burning fossil fuels and deforestation. In order to reduce the high levels of carbon dioxide in the atmosphere, the use of clean fuels in addition to more efficient techniques for carbon capture have been proposed. In this context, natural gas (NG) emerges as a great alternative for application in automotive vehicles and industrial processes, since this fuel is available in large quantities and combustion gases from NG are much cleaner than other fossil fuels. However, there are several drawbacks in using NG in large-scale applications. One drawback is related to the high cost of storing and transporting natural gas [1]. Natural gas consists of about 95% methane – a gas that cannot be liquefied at ambient temperature since its critical temperature is about 191 K. Therefore, the technology of liquefied natural gas (LNG) is not convenient for application in automotive vehicles due to the cost and complexity of storage that uses cryogenic temperatures in the gas liquefaction process. Another technology used for the storage of natural gas is compressed natural gas (CNG). The main disadvantage of this technology is the high pressure used to store NG (20 MPa), which results in heavy and expensive tanks in order to support such high pressures [2].

* Corresponding author. Tel.: +55 85 3366 9355; fax: +55 85 3366 9969.
E-mail address: marcondes@ufc.br (F. Marcondes).

http://dx.doi.org/10.1016/j.applthermaleng.2015.05.091
1359-4311/© 2015 Elsevier Ltd. All rights reserved.

A promising technology for storing natural gas is adsorbed natural gas (ANG). Currently, microporous-activated carbon is the best adsorbent to be used in ANG vessels [3]. The adsorption of gas allows a reduction in pressure storage (3,5-4 MPa), while also having a storage capacity similar to that obtained with CNG. The reduction in the storage pressure allows the use of more efficient tanks in addition to reducing the cost of compressing the gas [4]. Pressure reduction would allow for lighter materials for manufacturing the tank, such as aluminum, as well as the use of different geometries other than cylindrical, which provides a greater versatility in the design of the storage system. Yet, two major drawbacks exist that currently prevents ANG technology to be used on a large scale. The first is related to the shape of the adsorption isotherm which prevents a linear response of the storage capacity relative to the pressure. The second is related to the negative impact of heat of adsorption in the process of charging and discharging the system.

During the charging step, the bed temperature increases, and therefore, the adsorbed mass decreases. Inversely, the bed temperature decreases and the mass retained in the vessel increases during the discharge. Ridha et al. [5] and Ridha et al. [6] showed these effects of the charging and discharging processes of ANG vessels, respectively. The heat of adsorption, during the process of charging and discharging, reduces the adsorption/desorption capacity of the ANG system; this reduction can reach nearly 25% of the capacity of the system under isothermal condition [7,8].

In order to minimize the effects of heat of adsorption on performance of ANG vessels, various solutions have been proposed in the literature [8–11]. However, these solutions require the insertion of accessories in the storage system that reduces the space available for gas storage and increases the design complexity of the vessel. The proposed solutions have serious limitations regarding the dissipation of the heat of adsorption due to the low thermal conductivity of the adsorbent. Santos et al. [12] and Santos et al. [13] suggested an approach to overcome the heat of adsorption for loading and discharging processes in ANG vessels. The approach uses forced convection between the gas and the adsorbent in order to increase the heat dissipation of the adsorption vessel, which reduces the negative impact of the adsorption heat on the performance of ANG vessels.

A crucial assumption in the study of ANG systems is that the natural gas consists of pure methane. In this case, large variations in the gas velocity and pressure are observed in the bed due to the intense mass transfer in the adsorbent. These variations affect the displacement of the mass and temperature fronts, and consequently, the saturation time of the ANG vessel. Taking into account the momentum balance in the modeling process is fundamental to the correct description of the charge dynamics of the ANG vessel. In this work, the fast charge of natural gas in a column of activated carbon, open on both sides, is investigated in order to optimize the adsorbed natural gas into the activated carbon column. A detailed discussion is presented to improve Santos et al. [12] analysis, where the assumption of constant velocity was considered in the development of the numerical model. In particular, the mass transfer and friction effects on the velocity and pressure profiles during the fast charge process will be a focus of discussion.

2. Mathematical model

Fig. 1 shows the configuration investigated. In order to perform the analysis, a single column filled up with activated carbon and open on both sides is considered. The natural gas flows from one side of the column to the other. The constitutive equations are based on the mass, momentum, energy balances [14,15], and the ideal gas equation. Next, we show the model along with the initial and boundary conditions for the column and the adsorbent material.

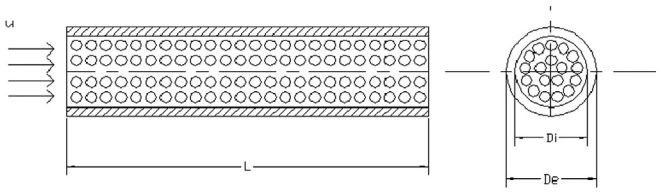

Fig. 1. Activated carbon-packed column.

2.1. Column model

For the column model, the following assumptions are considered:

- Radial effects are neglected.
- Natural gas is constituted of pure methane.
- Sorbate behaves as an ideal gas.

Under the above assumptions, the column model is constituted by the continuity equation, momentum equation, energy equation, and the ideal gas equation. The respective equations follow below:

$$\frac{\partial \rho_f}{\partial t} + \frac{\partial}{\partial x}\left(\rho_f u\right) = -\frac{1-\varepsilon}{\varepsilon}\frac{\partial \overline{q}}{\partial t}, \tag{1}$$

$$\frac{\partial}{\partial t}\left(\rho_f u\right) + \frac{\partial}{\partial x}\left(\rho_f\, u\, u\right) = -\frac{\partial p}{\partial x} - \frac{150\mu}{d_p^2}\frac{(1-\varepsilon)^2 u}{\varepsilon^2} - \frac{1.75\rho_f}{d_p}\frac{(1-\varepsilon)u^2}{\varepsilon}, \tag{2}$$

$$\frac{\partial}{\partial t}\left(\rho_f T_f\right) + \frac{\partial}{\partial x}\left(\rho_f\ u\ T_f\right) = \frac{\partial}{\partial x}\left(\frac{\lambda_f}{cp_f}\frac{\partial T_f}{\partial x}\right) + \frac{6h_p}{d_p}\frac{(1-\varepsilon)}{\varepsilon cp_f}\left(T_s - T_f\right) + \frac{2U_g\left(T_\infty - T_f\right)}{\varepsilon R_i cp_f}, \tag{3}$$

$$\rho_f = \frac{p}{R_g T_f}, \tag{4}$$

where ρ_f is the density of gas (kg/m^3), p is the pressure (Pa), T is the temperature (K), λ is the thermal conductivity (W/m K), ε is the bed porosity, R_g is the ideal gas constant (J/kg K), c_p is the specific heat at constant pressure (J/kg K), d_p is the pellet diameter (m), U_g is the overall heat transfer coefficient (W/m^2 K), R_i is the internal column radius (m), and subscript f denotes the fluid phase.

In order to study the adsorption process, it is assumed that an overcooled gas stream with constant temperature (T_{in}) and pressure (p_{in}) is suddenly forced into an activated carbon-packed column, which is initially saturated with gas at a temperature (T_0) and a pressure (p_0). The initial conditions used in the adsorption step are the last values of temperature and pressure obtained at the ending of the desorption process. The outlet pressure is kept at p_0. Details of the methane desorption in activated carbon can be found in Santos et al. [13]. Therefore, the following initial and boundary conditions are applied to the bed equations:

$$p(x, t=0) = p_0; \quad T_f(x, t=0) = T_0; \quad u(x, t=0) = u_0, \tag{5}$$

$$p(x=0,t)=p_{in};\quad T_f(x=0,t)=T_{in}, \tag{6}$$

$$p(x=L,t)=p_0;\quad \frac{\partial T_f(x=L,t)}{\partial x}=0. \tag{7}$$

2.2. Pellet model

The following assumptions are applied to the pellets:

- Pellets are considered to be spherical particles that are uniformly distributed.
- The monodisperse model describes the adsorption kinetics in the adsorbent; the effective mass diffusion coefficient is considered constant.
- Temperature is uniform inside the adsorbent particles.
- Adsorption equilibrium is assumed in the external surface of the adsorbent particles.

Using the above assumptions, the mass and energy balance equations for the pellet are respectively given by

$$\frac{\partial q}{\partial t}=\frac{1}{r^2}\frac{\partial}{\partial r}\left(r^2 D_{ef}\frac{\partial q}{\partial r}\right), \tag{8}$$

and

$$C_s\frac{\partial T_s}{\partial t}=\frac{6h_P}{d_P}\left(T_f-T_S\right)+(-\Delta H)\frac{\partial \overline{q}}{\partial t}, \tag{9}$$

where q denotes the concentration of gas in the solid phase (kg/m^3), r is the radius (m), D_{ef} is the effective mass diffusion coefficient (m^2/s), ΔH is the heat of adsorption (J/kg), $\overline{q}$ is the volumetric average concentration of the gas in the adsorbent particle (kg/m^3), h_p is the convection heat transfer coefficient in the pellet surface (W/m^2 K), and the subscript S denotes the solid phase.

The initial and boundary conditions for the pellet equations are given by

$$q(r,t=0)=q^*(p_0,T_0);\quad T_S(t=0)=T_0, \tag{10}$$

$$\frac{\partial q(r=0,t)}{\partial r}=0, \tag{11}$$

$$q(r=R_P,t)=q^*(p,T_S), \tag{12}$$

where q* is relative at the adsorption equilibrium.

2.3. Determination of the heat transfer coefficients

The fluid-particle heat transfer coefficient h_p is given by the following correlation described in Ruthven [14]:

$$Nu_p=\frac{h_p d_p}{\lambda_f}=2+1.1\mathrm{Pr}^{1/3}\mathrm{Re}^{0.6}. \tag{13}$$

The overall heat transfer resistance in the column wall is given by the sum of the inner convective resistance, wall conductive resistance, and outer convective resistance. Therefore, the overall heat transfer coefficient U_g is given by

$$U_g=\frac{1}{\frac{1}{h_i}+\frac{R_i}{\lambda_w}\ln\left(\frac{R_e}{R_i}\right)+\frac{R_i}{R_e}\frac{1}{h_e}}. \tag{14}$$

The inner convective coefficient is given by Ruthven [14]:

$$Nu_i=\frac{h_i D_i}{\lambda_f}=0.813\mathrm{Re}^{0.19}\exp(-6\mathrm{d_p}/D_i) \tag{15}$$

Forced convection conditions were assumed to evaluate the external convective coefficient. The external convective coefficient is given by the following correlation described in Incropera and DeWitt [16]:

$$Nu_e=\frac{h_e D_e}{\lambda_{air}}=0.193\mathrm{Re}^{0.618}\mathrm{Pr}^{1/3}. \tag{16}$$

3. Numerical procedure

The equations for the column model and the mass balance equation for the pellet are solved by the finite-volume method [17,18]. The pressure–velocity coupling was treated by the Implicit Pressure Explicit Momentum (PRIME) method [19], while the staggered arrangement was used to store the variables in the computational grid. The Weight Upwind Differencing Scheme (WUDS) by Raithby and Torrance [20] is utilized to evaluate the physical properties in the interfaces of each control volume. In each time-step, an iterative procedure is performed in order to treat the non-linearities and coupling between equations. The linear systems are solved by the tri-diagonal matrix algorithm. We used the procedure suggested by Marcondes and Maliska [21] in order to evaluate the velocities in the inlet and outlet of the column. Subsequently, the gas temperature is obtained by the energy equation and the gas density by the ideal gas law. For the pellets, the mass and energy balances are used to determine the volumetric average concentration and temperature, sequentially. It is important to mention that the last two variables are the respective source terms to the column model for the mass and energy balances. The simulations were performed using 100 volumes for the column and 10 volumes for the pellets. When more refined grids were used, the results were not significantly altered. Note that all simulations were performed using a constant time-step equal to 5×10^{-4} s. The iterative procedure to obtain the solution in each time-step involves the following steps:

1) Supply the initial values of the variables p,u, T_f, q, and T_S.
2) Solve Eq. (8) for each control volume of the column and obtain the average concentration inside each pellet.
3) Solve Eq. (9) for each control volume of the column and obtain the temperature inside each pellet.
4) Calculate the pressure field through continuity Equation.
5) Calculate the velocity field through momentum Equation.
6) Calculate the temperature field through energy Equation.
7) Calculate the density field through ideal gas law.
8) Return to step 2 and iterate until convergence is reached at the current time level.
9) Progress to the next time level.

The following convergence criteria verified the convergence of the solution in each time-step:

$$\left|\frac{\varphi_P^{k+1}-\varphi_P^k}{\varphi_{\max}-\varphi_{\min}}\right|\le 10^{-5} \tag{17}$$

Here, $|\varphi_{\max}-\varphi_{\min}|$ represents the maximum variation of the gas density at the k-th iteration. When Eq. (17) is not satisfied for each control volume, an additional iteration is required.

4. Results and discussion

It is helpful to discuss the numerical validation of the developed computational code prior to presenting the results of the current

investigation. Malek and Farooq [22] conducted a detailed investigation about the adsorption and desorption processes of diluted methane in activated carbon. In their work, experimental data for the breakthrough curves of methane, ethane, and propane in conjunction with activated carbon and silica gel were determined for three temperatures (299.15, 318.15, 338.15 K), two particle sizes (0.129, 0.258 cm), various gas velocities (1.3–4.3 cm/s), and various feed pressures (1.99–6.41 bar).

Helium was used as a carrier gas in the diluted mixture. In order to validate our approach, we selected Case Study 3 from the work of Malek and Farooq [22]. This case study presents the breakthrough curves for the adsorption and desorption of methane in activated carbon. The results for a mixture of methane (5%) and helium (95%) in terms of breakthrough curves for desorption and adsorption processes are shown in Fig. 2 of Malek and Farook's study [22]. The following pressure, temperature, and velocity were used in the experiment: 2.4848 bar, 299.15 K, and 1.56 cm/s. A stainless steel column with an internal diameter of 3.5 cm and a length of 40 cm was used for the adsorption and desorption tests.

To simulate the experiment conducted by Malek and Farooq [22], we added an equation similar to Eq. (1) for the methane plus helium mixture. Fig. 2 shows a comparison of the breakthrough curves obtained in this work with the experimental results of Malek and Farook [22] for the adsorption and desorption of methane in activated carbon. The optimal adjustment between the experimental and numerical results was obtained when the effective mass diffusion coefficient was set to 10×10^{-3} cm^2/s Fig. 3 shows a comparison of the temperature profiles obtained in the present work with the experimental profiles from Malek and Farooq [22] at the mid-point and outlet of the column for the adsorption test. Moreover, the optimal adjustment between the experimental and numerical results was obtained when the overall heat transfer coefficient in the column wall was set to 25 W/(m^2 K). Figs. 2 and 3 illustrate a good agreement between the numerical and experimental results; therefore, we assume that the developed computational code represents the dynamics of methane adsorption in activated carbon. Santos et al. [13] offers a discussion in greater detail of the numerical validation process and the developed computational code as well as Malek and Farook's [22] experiment.

4.1. Numerical results

The geometrical dimensions of the column and other data used in the simulations presented in this section are shown in Table 1. The packed adsorbent used in the column is G216 of North American Carbon Coal, Inc., of Columbus, Ohio. The adsorption equilibrium is given by the Langmuir isotherm. The fitting parameters of the isotherm were obtained from experimental data published by Remick and Tiller [23].

$$q^*(p, T_s) = \frac{q_m b p}{1 + bp}, \tag{18}$$

with

$$q_m = 55920\, T_s^{-2.3}, \tag{19}$$

$$b = 1.0863 \times 10^{-7} \exp(806/T_s). \tag{20}$$

Activated carbon has a high diffusion constant, $D_{ef}/R_p^2 \cong 10^{-1}$ s^{-1} [24] for the adsorption of methane. Consequently, activated carbons typically provide low resistance to mass diffusion. Fig. 4 shows the velocity profiles for an imposed pressure drop equal to 700 Pa. The inlet gas temperature is equal to 30 °C and the initial temperature was considered equal to 400 °C, which corresponds to the final temperature of the conclusion of the desorption process. From the profiles shown in Fig. 4, we observe a sharp growth of the gas velocity in the mass transfer zone. However, prior to and following this zone, the gas velocity remains constant. Therefore, the adsorption process largely impacts the gas velocity in the region where mass transfer occurs. The gas velocity is constant for the entire column after 800 s when the adsorption process is completed. Fig. 5 presents the effect of the pressure drop on the adsorption process. Initially, before the adsorption starts, the pressure gradient is almost constant for the whole column. However, after the adsorption evolves through the column, the pressure

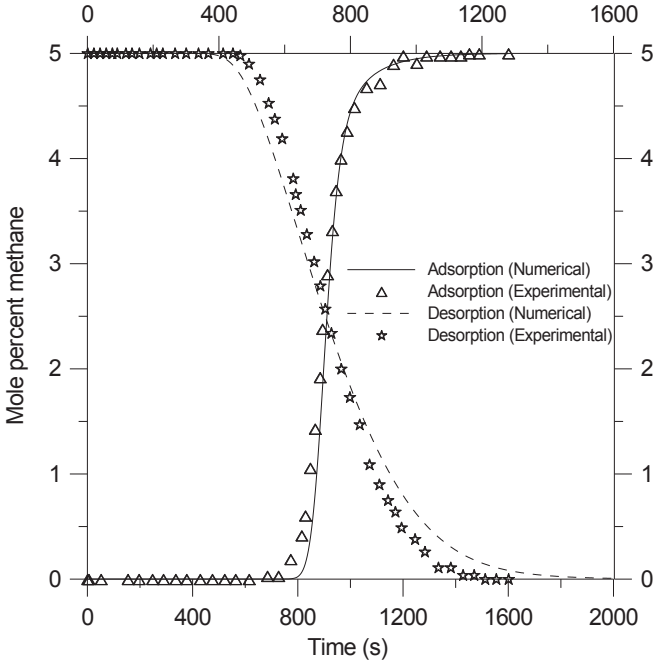

Fig. 2. Comparison of the experimental and simulated breakthrough curves.

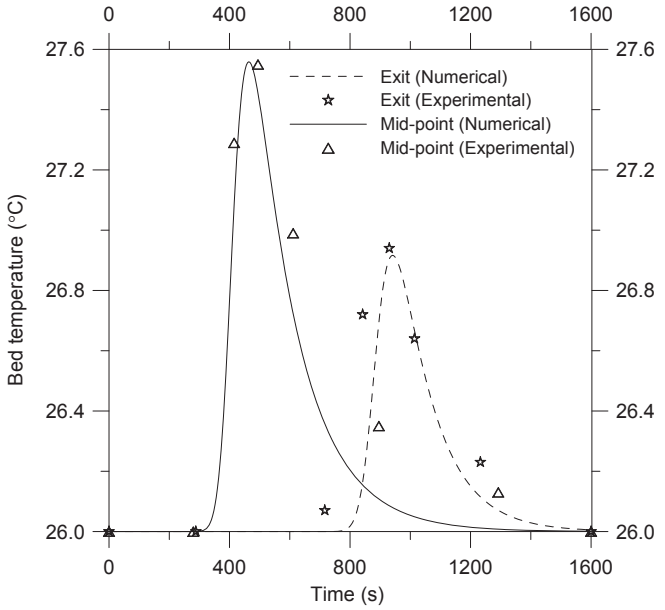

Fig. 3. Comparison of the experimental and simulated temperature profiles.

Table 1
Data and physical properties utilized in the simulations.

Particle radius, Rp	0.5 mm
Column length, L	0.5 m
Column inner radius, R_i	2.5 cm
Initial pressure, p_0	3.5 MPa
Initial temperature, T_0	400 °C
Pressure drop, $dp = p_{in} - p_{out}$	400, 700, 1000, 1300 Pa
Inlet temperature, T_{in}	0, 30, 50, 100 °C
Mass diffusion coefficient, D_{ef}	2.5×10^{-8} m^2/s, Cess [20]
Ideal gas constant, R_g	518.35 J/kg K
Bed porosity, ε	0.4
Adsorbent density, ρ_s	2150 kg/m^3, Mota [1]
Adsorbent specific heat, C_{ps}	648 J/kg K, Mota [1]
Effective thermal conductivity of the bed, λ_{ef}	0.2 W/m K, Mota [3]
Sorbate specific heat, C_{pg}	2450 J/kg K, Mota [1]
Surrounding temperature, T_∞	300.3 K
Adsorption heat, ΔH	-1.1×10^6 J/kg, Mota [1]
Wall thickness	0.4 cm
Wall thermal conductivity	15.1 W/m K

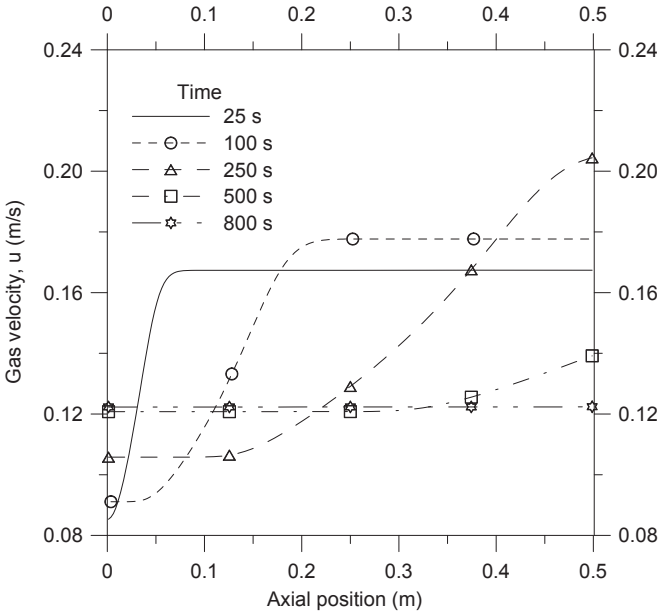

Fig. 4. Axial velocity profiles.

gradient increases due to mass transfer. Finally, a constant pressure gradient is observed after 800 s for the whole column, indicating the ending of the adsorption process.

The increase in the pressure gradient due to the adsorption can be explained based on the increase in the gas velocity within the mass transfer zone. Outside this zone, both the pressure gradient and velocity remain constant. This information is presented in Fig. 6, which shows the effect of gas adsorption on the pressure gradient. Fig. 7 shows the evolution of the thermal front in to the column, while Fig. 8 presents the adsorption front. As the cold gas front evolves, the temperature at each point in the column decreases to the minimum value. This value corresponds to the equilibrium condition with the injected cold gas. Moreover, due to the inverse dependence of the adsorption equilibrium with the temperature, the adsorbed mass increases to its maximum value when the mass front moves forward into the column. Fig. 9 presents the density profiles in the column. Due to the low pressure drop applied in the column, the gas density varies strongly with the temperature. When the column reaches its minimum temperature, the gas density reaches its maximum value according to the ideal gas law.

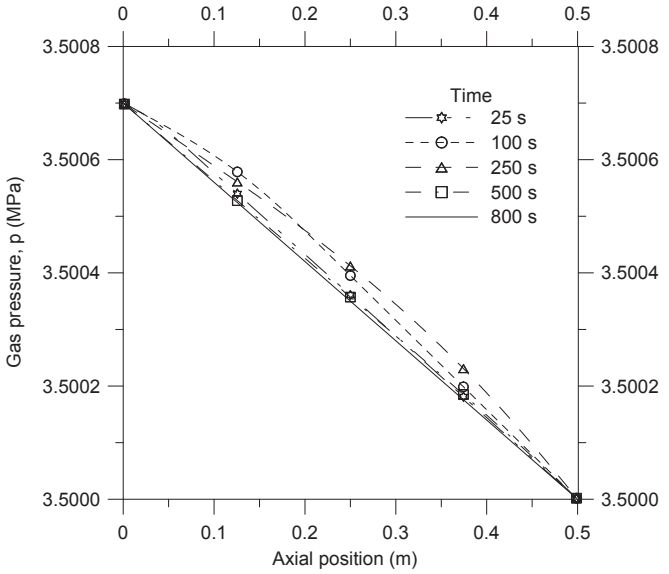

Fig. 5. Axial pressure profiles.

4.1.1. Influence of the inlet temperature in the performance of the adsorption process

The inlet temperature can have a large effect on the adsorption of natural gas in activated carbon. Fig. 10 shows the evolution of the average temperature of the adsorbent bed versus time for three inlet temperatures studied: 0, 50 and 100 °C. The average bed temperature was observed to decrease until it reached the corresponding inlet temperature. In addition, reducing the inlet temperature was observed to decrease the average temperature of the adsorbent bed. Fig. 11 shows the effect of the inlet temperature on the adsorbed mass. From this figure, it is possible to observe that decreasing the inlet temperature increases the amount of adsorbed gas into the column at the end of the adsorption process.

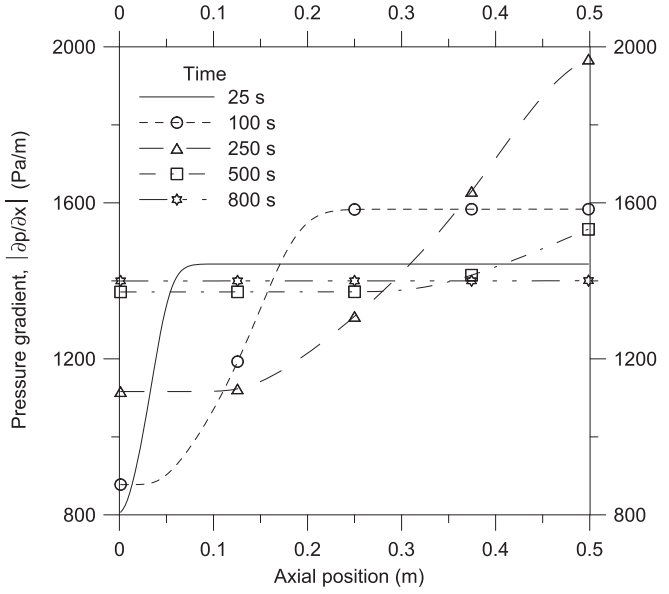

Fig. 6. Pressure gradient profiles.

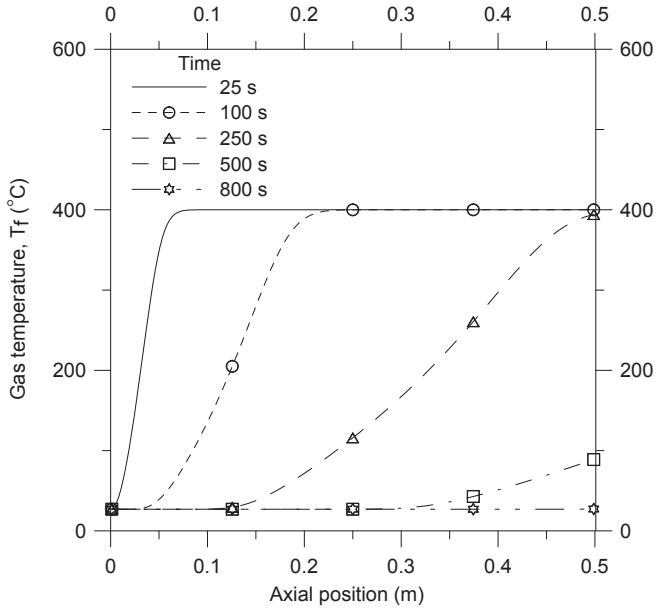

Fig. 7. Temperature profiles.

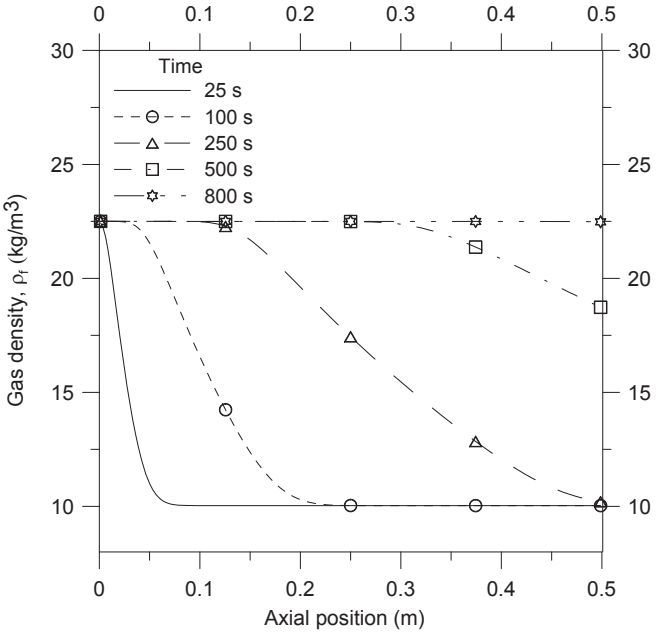

Fig. 9. Density profiles.

4.1.2. Influence of pressure drop on the performance of the adsorption process

In this section, the effect of the pressure drop between the inlet and outlet of column to the adsorption of natural gas in activated carbon bed is investigated. Fig. 12 shows the effect of pressure drop on the average temperature of the adsorbent bed. Four pressure drops were considered: 400, 700, 1000, and 1300 Pa. Fig. 12 shows that when the pressure drop is progressively increased, the time to reach steady-state conditions decreases. The effect of pressure drop to the adsorbed mass is shown in Fig. 13. From this figure, it is possible to observe that increasing the pressure drop reduces the time required for the complete adsorption of the column. It is also observed that the adsorption time can vary between 500 and 1000 s, depending on the applied pressure drop. These times are considered satisfactory for the fast-filling process of the column. The reduction of the time necessary to reach equilibrium state, observed in Figs. 12 and 13, occurs because the gas velocity increases as the applied pressure drop is increased.

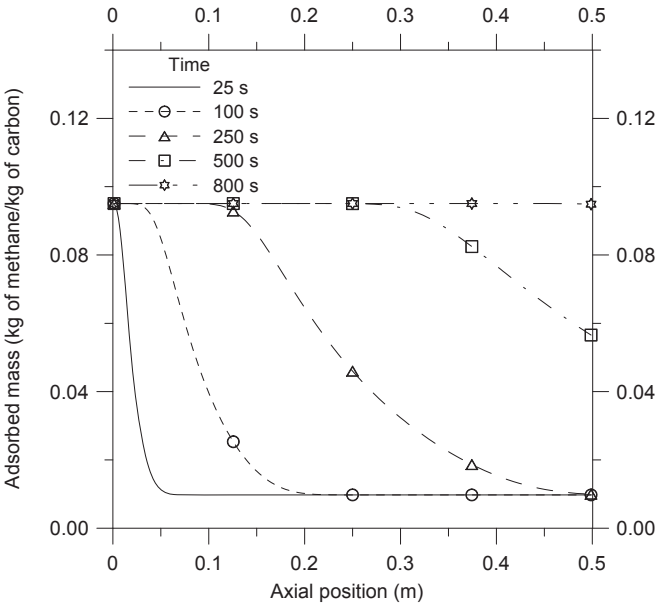

Fig. 8. Adsorbed mass profiles.

5. Alternative solution to the fast charge in ANG vessels

The numerical results obtained in this work in conjunction with an adsorbent column open on both sides indicate that the reduction in the gas inlet temperature was observed to increase the mass adsorbed in the column. It was also observed that increasing the applied pressure drop to the column reduces the adsorption time. Santos et al. [12] proposed an alternative solution for the fast charge in ANG vessels that takes advantage of the numerical results of the present study. This solution utilizes a new tank configuration that consists of several tubes packed with activated carbon. The solution's implied outcome of using forced convection between the adsorbent grains and the gas flow is to increase the heat transfer into the bed. All non-adsorbed natural gas that leaves the tank passes through an external heat exchanger, which removes the adsorption heat generated during the charge process. Finally, the cooled gas is recirculated to the tank through a compressor to facilitate the charge process in the adsorbent bed. Depending on the working conditions of the heat exchanger, the overcooled gas enters into the tank, and hence, increases the adsorbed mass. The compressor can also be optimized to provide the pressure drop that minimize the charging time of the tank. The advantage of the new proposed system is the use of forced convection inside the vessel in order to intensify the heat exchange into the system, reducing the negative effects of heat of adsorption in ANG vessels.

6. Conclusions

This work presents a numerical investigation of the dynamics of adsorption of pure methane in a packed column with activated

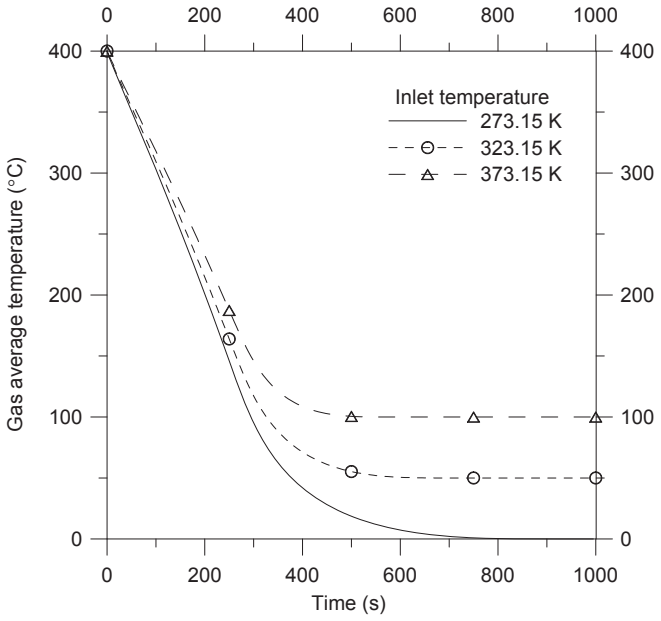

Fig. 10. Effect of the inlet temperature on the average temperature of the bed.

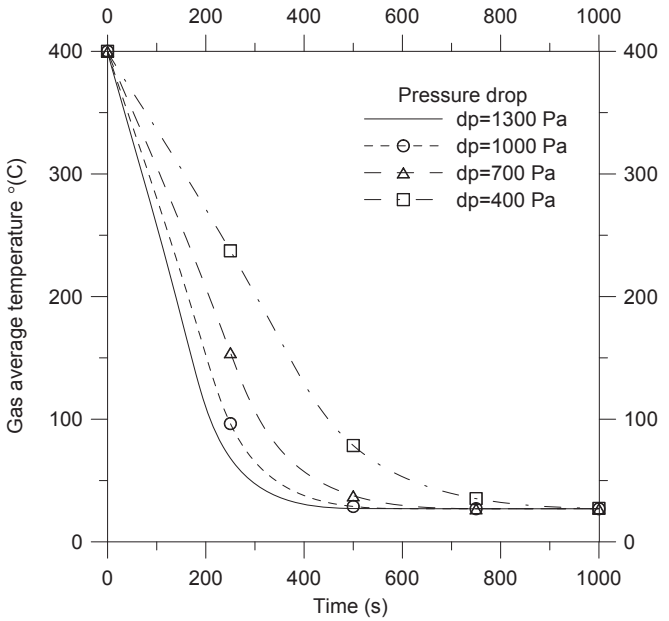

Fig. 12. Influence of the applied pressure drop on the average temperature of the bed.

carbon in order to optimize the fast charge process in ANG vessels. The mathematical model is described by the mass, momentum, and energy balances in conjunction with the ideal gas equation. A computer code based on the finite-volume method was developed to solve the system of equations describing the dynamics of the charge process. The numerical results show that the progressive reduction of the inlet temperature of the gas increases the adsorbed mass, and therefore, improves the performance of the charge process. The results also show that the time required for the full charge is a function of the applied pressure drop in the column. An alternative solution to the fast charge in ANG vessels was presented in order to reduce the negative effects of heat adsorption during the charge process.

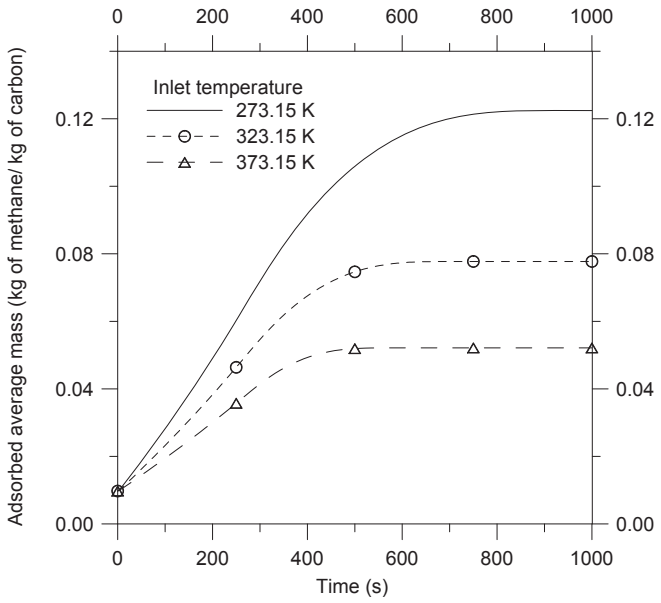

Fig. 11. Influence of the inlet temperature on the average adsorbed mass.

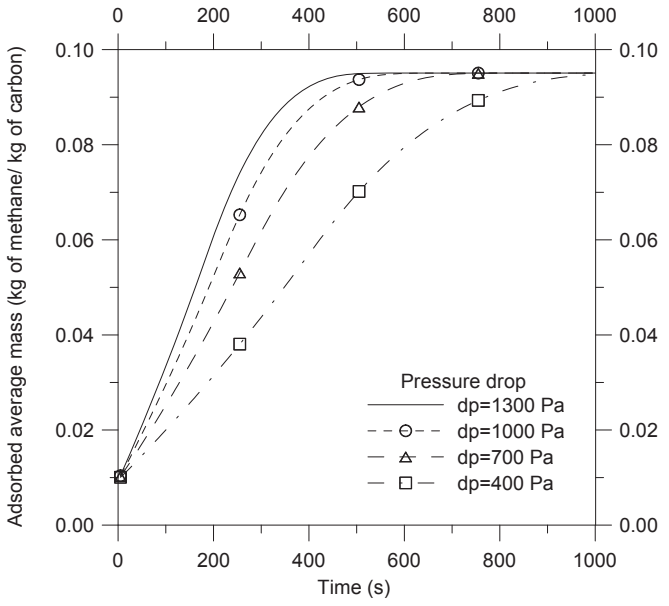

Fig. 13. Influence of the applied pressure drop on the average adsorbed mass.

Acknowledgements

The authors thank the CNPq (The National Council for Scientific and Technological Development of Brazil) and FUNCAP (The Foundation to Support the Scientific and Technological Development of Ceará-Brazil) for their financial support through grants (305443/2012-4 and 305415/2012-3) and (BP1-0067-00162.01.00/12), respectively.

References

[1] O. Talu, An overview of adsorptive storage of natural gas, in: Proceedings of international conference on fundamentals of adsorption, 1992, pp. 655–662. Kyoto, Japan.

[2] J.P.B. Mota, E. Saatdjian, D. Tondeur, A simulation model of a high-capacity methane adsorptive storage system, Adsorption 1 (1995) 17–27.
[3] D. Lozano-Castelló, J. Monge-Alcañiz, M.A. Casa-Lillo, D. Cazorla-Amorós, Advances in the study of methane storage in porous carbonaceous materials, Fuel 81 (2002) 1777–1803.
[4] H. Najibi, A. Chapoi, B. Tohidi, Methane/natural gas storage and delivered capacity for activated carbons in dry and wet conditions, Fuel 87 (2008) 7–13.
[5] F.N. Ridha, R.M. Yunus, M. Rashid, A.F. Ismail, Thermal analysis of adsorptive natural gas storages during dynamic charge phase at room temperature, Exp. Therm. Fluid Sci. 32 (2007) 14–22.
[6] F.N. Ridha, R.M. Yunus, M. Rashid, A.F. Ismail, Thermal transient behavior of an ANG storage during dynamic discharge phase at room temperature, Appl. Therm. Eng. 27 (2007) 55–62.
[7] S.C. Hirata, P. Couto, L.G. Lara, R.M. Cotta, Modeling and hybrid simulation of slow discharge process of adsorbed methane tanks, Int. J. Therm. Sci. 48 (2009) 1176–1183.
[8] K.J. Chang, O. Talu, Behavior and performance of adsorptive natural gas storage cylinders during discharge, Appl. Therm. Eng. 16 (1996) 359–374.
[9] L.L. Vasiliev, L.E. Kanonchik, D.A. Mishkinis, M.I. Rabetsky, Adsorbed natural gas storage and transportation vessels, Int. J. Therm. Sci. 39 (2000) 1047–1055.
[10] X.D. Yang, Q.R. Zheng, A.Z. Gu, X.S. Lu, Experimental studies of the performance of adsorbed natural gas storage system during discharge, Appl. Therm. Eng. 25 (2005) 591–601.
[11] J.P.B. Mota, I.A.A.C. Esteves, M. Rostam-Abadi, Dynamic modelling of an adsorption storage tank using a hybrid approach combining computational fluid dynamics and process simulation, Comput. Chem. Eng. 28 (2004) 2421–2431.
[12] J.C. Santos, F. Marcondes, J.M. Gurgel, Performance analysis of a new tank configuration applied to the natural gas storage systems by adsorption, Appl. Therm. Eng. 29 (2009) 2365–2372.
[13] J.C. Santos, J.M. Gurgel, F. Marcondes, Analysis of a new methodology applied to the desorption of natural gas in activated carbon vessels, Appl. Therm. Eng. 73 (2014) 929–937.
[14] D.M. Ruthven, Principles of Adsorption and Adsorption Processes, Wiley Interscience, New York, 1984.
[15] R.T. Yang, Gas Separation by Adsorption Processes, Butterworth, Boston, 1987.
[16] F.P. Incropera, D.P. DeWitt, Fundamentals of Heat and Mass Transfer, fourth ed., John Wiley & Sons, 1996.
[17] C.R. Maliska, Computational Fluid Mechanics and Heat Transfer, LTC, Rio de Janeiro, Brazil, 2004 (in Portuguese).
[18] S.V. Patankar, Numerical Heat Transfer and Fluid Flow, Hemisphere, 1980. New York.
[19] C.R. Maliska, A Solution Method Three-dimensional Parabolic Fluid Flow Problems in Nonorthogonal Coordinates, University of Warterloo, Warterloo, Canada, 1981 (Ph. D. thesis).
[20] G.D. Raithby, K.E. Torrance, Upstream-weight differencing schemes and their application to elliptic problems involving fluid flows, Comput. Fluids 2 (1974) 191–206.
[21] F. Marcondes, C.R. Maliska, Treatment of the inlet boundary conditions in natural convection flows in open-ended channels, Num. Heat. Transf. Part B 35 (1999) 317–345.
[22] A. Malek, S. Farooq, Kinetics of hydrocarbon adsorption on activated carbon and silica gel, AIChE J. 43 (1997) 761–776.
[23] R.J. Remick, A.J. Tiller, Heat generation in natural gas adsorption systems, Vancouver, Canada, in: Gaseous Fuels for Transportation International Conference, 1996.
[24] R.D. Cess, Handbook of Heat Transfer, McGraw-Hill, New York, 1973.

Nomenclature

C_p: specific heat at constant pressure (J/kg K)
C_S: volumteric heat capacity of the adsorbent (J/m^3 K)
d_p: pellet diameter (m)
D_{ef}: effective mass diffusion coefficient (m^2/s)
q: concentration of the gas in adsorbent (kg/m^3)
$\bar{q}$: volumetric average concentration over pellet (kg/m^3)
u: interstitial velocity (m/s)
h: convection heat transfer coefficient (W/m^2 K)
ΔH: heat of adsorption (J/kg)
L: column length (m)
Nu: Nusselt number
p: gas pressure (Pa)
pr: Prandtl number
r: pellet radial coordinate (m)
R: column radius (m)
Re: Reynolds number
R_g: ideal gas constant (J/kg K)
t: time (s)
T: temperature (K)
U_g: overall heat transfer coefficient (W/m^2 K)
x: axial coordinate in column (m)

Greek letters

ε: bed porosity
λ: thermal conductivity (W/m K)
ρ: specific mass (kg/m^3)

Subscripts

∞: relative to the ambient
0: relative to the initial condition
e: relative to the external surface
f: relative to the fluid phase
in: relative to the column inlet
p: relative to the pellet
S: relative to the solid phase
w: relative to the column wall

Superscripts

*: relative to the adsorption equilibrium